Journal of Computational Science 45 (2020) 101173

Contents lists available at ScienceDirect

Journal of Computational Science

journal homepage: www.elsevier.com/locate/jocs

A passenger model for simulating boarding and alighting in spatially confined transportation scenarios

Boyi Su[a,b,*], Philipp Andelfinger[a,b], Jaeyoung Kwak[b], David Eckhoff[a,c], Henriette Cornet[a], Goran Marinkovic[a], Wentong Cai[b], Alois Knoll[b,c]

[a] TUMCREATE Ltd, 1 10-02 Create Way, CREATE Tower, Singapore
[b] Nanyang Technological University, 50 Nanyang Ave, Singapore
[c] Technische Universität München, Arcisstraße 21, 80333 München, Germany

ARTICLE INFO

Article history:
Received 8 January 2020
Received in revised form 22 May 2020
Accepted 18 June 2020
Available online 3 August 2020

Keywords:
Agent-based simulation
Social force model
Confined space
Autonomous vehicle
Recognition-primed decision (RPD)
Dwell time evaluation

ABSTRACT

Crowd simulation has been widely used as a tool to demonstrate the behavior of passengers on public transport. A simulation model allows researchers to evaluate the platform or interior designs without involving real-world experimentation. In this paper, we propose a passenger model to measure the effect of different public transport vehicle layouts on the required time for boarding and alighting. We first model a low level collision avoidance behavior based on an extended social force model aiming at simulating human interactions in confined spaces. The model introduces a mechanism to emulate rotation behavior while avoiding complex geometric computations and is calibrated to experimental data. The model also allows agents to perform collision prediction in low density environments. Strategical behavior of passengers is modeled according to the recognition-primed decision paradigm and combined with the collision avoidance model. We validate our model against real-world experiments from the literature, demonstrating deviations of less than 6%. In a case study, we evaluate the boarding and alighting times required by three autonomous vehicle interior layouts proposed by industrial designers in both low-density and high-density scenarios.

1. Introduction

The introduction of autonomous vehicles as a mode for public transport offers promising benefits and can play an important role in reducing commute times for all passengers. One of the key challenges is to reduce the time required for passengers to board and alight these vehicles as too long dwell times would annul all time gains achieved through platooning or traffic light prioritization. The layout of these vehicles (e.g., the number, spacing and orientation of seats or the number, location, and size of doors) directly affects this dwell time and is therefore a critical property of autonomous public transport vehicles.

Ideally, once industrial designers have finalized a number of candidate AV layouts, real-world trials with mock-ups would be carried out to obtain a quantitative comparison. Unfortunately, this is often not feasible due to their cost-intensive and time-consuming nature, requiring a different mock-up for each design and a large number of participants to produce meaningful results. While virtual reality solutions can replace physical mock-ups, they introduce new challenges such as passenger interaction and uncertainties about the required level of immersion [7].

One possible solution is to instead use an agent-based model of the boarding and alighting behavior of passengers which can be used for the AV design evaluation. However, unlike the scenarios presented in many common agent-based simulation studies (e.g., [6,11]), the confined spaces inside a vehicle limits the movement of passengers. More complex actions including detour and body rotation are to be executed by a passenger to avoid collision with obstacles and other passengers. Achieving realistic navigation behavior in such scenarios therefore becomes the prior issue for the model development.

In our previous study [27], we presented a passenger model and tool aiming at solving the mentioned issues. We proposed an agent-based model to evaluate the boarding and alighting times with respect to given vehicle interior layouts. We proposed adaptations of well-known pedestrian simulation models to support the navigation in spatially confined scenarios. A novel size adaptation method was proposed to allow agents to navigate through nar-

* Corresponding author at: Nanyang Technological University, 50 Nanyang Ave, Singapore.
E-mail addresses: bsu@ntu.edu.sg (B. Su), philipp.andelfinger@gmail.com (P. Andelfinger), jaeyoung.kwak@ntu.edu.sg (J. Kwak).

https://doi.org/10.1016/j.jocs.2020.101173
1877-7503/

row corridors successfully without the need for complex geometric computations. The passenger behavior on the strategical level was carefully modeled according to the recognition-primed decision [19] framework as a set of so-called experiences [22].

Although the model has been put into practical use and acquired reasonable results, several open aspects and unsolved issues remained: the proposed size adaptation method lacked calibration to empirical data; the model has not considered the competitive behavior between passengers of the same priority level, e.g., two passengers boarding at the same time; the model has not been used for evaluating the layouts in high-density scenarios.

To address the aspects above, an extension of the previous research is presented in this paper. The main contributions can be summarized as follows:

- The model is further enhanced to tackle the challenges when agents move in spatially confined scenarios.
- The size adaptation method is improved by introducing gap maintenance and speed adjustment, both of which are investigated and calibrated with data from real-world experiments from the literature.
- A collision prediction algorithm is introduced to produce fast solutions of coming collisions of neighbors in low-density environments.
- Validation has been carried out through comparison to real-world experiments from the literature using the enhanced passenger model.
- Additional evaluations are presented with respect to several different AV layouts in both low density and high density scenarios.

The remainder of this paper is organized as follows: Section 2 introduces existing works fundamental to our model and related work in passenger simulation for public transport scenarios. In Section 3, we describe the behavior modeling in scenarios involving narrow corridors and the corresponding calibration. Section 4 describes our basic simulation scenario and Section 5 describes our proposed passenger model. In Section 6, we provide validation and performance evaluation results. Finally, Section 7 concludes the paper.

2. Background and related work

In this section, we outline the models used to represent the high-level decision making and the low-level collision-avoidance behavior of agents. Further, we discuss related work on agent-based simulation of public transport scenarios.

2.1. Recognition-primed decision

Decision making is an essential cognitive process in daily life. The traditional analytical decision-making models such as prescriptive analytical decision-making and rational choice model aim to acquire the optimal solution to a particular problem. However, such models are mainly based on laboratory experiments and fail to represent the actual process in reality, especially under time pressure [13].

Naturalistic decision making (NDM) models provide better representation on the fact that a human tends to make decisions based on estimations and guesswork rather than using purely rational processes [21]. In this paper, we use one of the most well-known NDM models, recognition-primed decision (RPD), as the conceptual framework for our model. Each agent maintains a repertoire of patterns representing its previous experiences. When encountering a problem, the agent selects a matching situation from its repertoire and predicts the expected outcome based on the previous experience. A comprehensive description of RPD is given in [19]. In Section 5, we describe how the concepts of RPD are applied to our specific modeling problem.

Our agent-based model relies on the implementation of RPD in the CrowdTools simulation framework, which encapsulates the decision-making logic into experiences composed of one or more stages [22]. The decision-making process consists of three iterative steps:During *situation assessment*, the agent perceives situational cues, which are used to update its emotional state. During *experience matching*, the agent selects from its repertoire the experience that is the most similar to the current situation. During *experience execution*, the actions associated with the selected experience are carried out.

Four cognitive components implement the following tasks involved in the above process: The *perception system* detects the constraints imposed by the virtual environment and filters the relevant information for the decision making. The *working memory* stores predefined information and situational states. The *decision system* carries out the decision making based on the information from the perception system and the working memory. Finally, the *action system* executes the actions determined by the decision system.

2.2. Collision avoidance

Microscopic crowd simulations represent humans as autonomous agents that sense their surroundings, make decisions and carry out corresponding actions. The social force model (SFM) [23] is a popular and well-studied model of the distance-keeping behavior of pedestrians. We choose the SFM for the basic collision avoidance due to its low computational cost and ease of implementation. The SFM models the intention of a pedestrian as a driving force and the resistance between a pedestrian and its surrounding objects, i.e., neighboring pedestrians and stationary obstacles, as repulsive forces. The force acting on an agent i at time t is defined as follows:

$$m_i \frac{\mathrm{d}v_i}{\mathrm{d}t} = m_i \frac{v_i^0(t) - v_i(t)}{\tau_i} + F_{nb} + F_{obs}$$

The first summand represents the driving force, where m_i is the mass of the agent, $v_i^0(t)$ is the preferred velocity and $v_i(t)$ is the actual velocity; F_{nb} is the net force from neighboring agents, and F_{obs} is the force from the surrounding obstacles. The force received from neighbor j is defined as $f_{ij} = A\exp(-\frac{D_{ij}}{B})n_{ij}$. The time step size is denoted by τ_i. The parameters A, B determine the strength and range of the force. D_{ij} is the distance between the agent i and agent j. n_{ij} is the direction vector pointing from the position of agent i denoted by P_i to the position of agent j denoted by P_j. The force from an obstacle line l is determined in the same fashion based on the distance of agent i to the closest point on l.

Following the above definitions, for a pair of agents, the SFM defines a pair of opposite forces, which can lead to undesirable symmetric interactions [17]. As an example, suppose two agents are heading exactly towards each other in an open space. The agents experience forces opposite to their velocity, and decelerate without changing direction, leading to a standstill or collision. To solve this issue, a variant of the SFM introduces a right-of-way mechanism based on agent priorities [12]. The parameter B in the original SFM is replaced by $B_{ij} = B + R_{ji}r_i$, with R_{ij} which reflects the right-of-way of agent i over agent j. Here, $R_{ij} = \max(1, p_i - p_j)$ is given as a function of agent i's and j's priorities, i.e., p_i and p_j. The value of R_{ij} becomes 1 if $p_i > p_j$, otherwise 0. The direction of the repulsive force is adapted according to R_{ij}. If agent i has higher priority than j, the repulsive force on j is assigned an angle between 0° and 90° to the preferred velocity of i.

2.3. Body representation in agent-based modeling

Many existing agent-based models rely on the traditional circular shape representation of agents. These models assume that the space occupied by a human in any direction is equal to their shoulder width and therefore overestimate the actual space occupied. They fail to support scenarios where an agent attempts to navigate through a path that is narrower than its shoulder width. To solve this issue by introducing lateral motion, some works propose elliptical [4,25] or even irregular polygonal representations [1,20]. However, these approaches substantially increase the complexity of the collision avoidance, both computationally and in terms of the need to address special cases, e.g., when there is insufficient space for an agent to rotate.

Another possible solution is to dynamically change the shape of an agent. Baglietto and Parisi [3] propose a model with circular agents, but allow the agents to scale their radius. A similar idea can be found in [9], where the agents are modeled as ellipses, with a scalable radius along the walking direction. However, in both methods, agents adapt their radius only according to their own walking speed and do not allow for dynamic adjustments to adapt to the current environment.

In our work, we propose a solution for the navigation in confined areas where agents representing by circles are able to perceive the surrounding environment and adapt their sizes according to specific rules.

2.4. Simulation of passengers in public transport scenarios

Several existing works have used agent-based simulations to determine the required dwell time of public transport vehicles. Perkins et al. [24] employ SFM to assess the dwell time of a train under various parameter combinations for the door width and placement as well as the crowd mix. Their focus is on the train-platform interface. Thus, in contrast to our work, the geometry and seat placement inside the vehicle as well as the passenger behavior after boarding are not considered.

Fletcher et al. [16] propose an automated procedure to optimize the geometry of a train's interior layout based on evolutionary algorithms and evaluation using agent-based simulation. While their approach provides interesting avenues for future research, the considered parameters of aisle width, seat width, and door width limit the range of possible layouts. The aim of our work is to support industrial designers when evaluating different layouts. Thus, we rely on color-coded floor plans as input so that designers are free in their decisions on aspects such as the seat placement and orientation and the placement of walls.

For parameterization and validation of passenger models, the existing works in the literature have relied on video footage [5,16,24,31], smart-card payment records [28], and experiments using mock-ups [18,26]. In our work, we validate against real-world experiments based on mock-ups from the literature. We are investigating data collection from virtual reality experiments [2] and real-world observations to achieve an accurate parameterization with respect to aspects such as the passengers' seat selection preferences.

3. Behavior modeling in confined space

In this section, we present a decision-making model initially aiming at a very simple scenario: two pedestrians traverse a narrow corridor of width w in opposite direction, which in a real-world situation would require rotation to avoid a collision (cf. Fig. 1). The model retains its reliance on the traditional SFM for basic collision avoidance. Size adaptation and collision prediction mechanisms are introduced to allow the agent to dynamically adjust their sizes and desired velocities according to the environment.

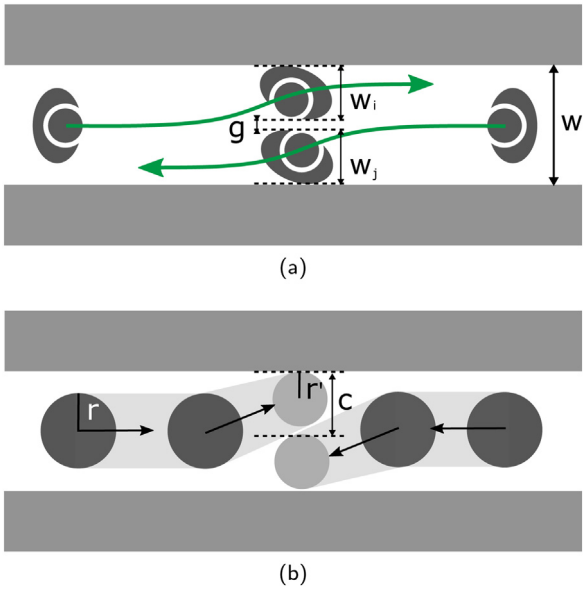

Fig. 1. A narrow corridor scenario with two pedestrians walking in opposite direction. (a) demonstrates the detour and rotation behavior in reality. (b) shows how our model imitates the pedestrians' real-world behavior through collision prediction and size adaptation.

3.1. Size adaptation

As discussed in Section 2.3, the original SFM relying on a circular representation of agents fails to support this scenario due to overestimating the actual space occupied by a human. We therefore propose a solution allowing agents for adapting their sizes to the confined navigation space.

Our modeling rationale is that in real-world situations, the rotation performed by passengers to travel through corridors reduces their effective size in perpendicular direction to their target. Thus, temporarily reducing the size of circular agents achieves a similar effect as a rotation of agents represented by more complex shapes, while avoiding the associated complexity.

As shown in Fig. 2(a), the agent first generates two detecting regions on left and right hand sides of his facing direction for corridor detection. The length of a detecting region is configured as the walking distance per second for a moving agent, or 1.5 times radius for an agent that is standing still. The width of a detecting region is configured as the agent radius plus 0.01 m.

Each region queries the objects (obstacle lines or agents) it is intersecting with, and stores the closest one to the agent.

A corridor is assumed to be present if an object is found on each side. However, it is considered obstructed if there is any other object simultaneously intersecting with both detecting regions (cf. Fig. 2(c)). When an unobstructed corridor is detected, the agent reduces its radius for a configurable amount of time (cf. Fig. 2(b)).

3.1.1. Gap maintenance

Unlike in our previous work [27], the new model allows an agent to determine a suitable radius based on the situation instead of relying on a fixed value. The clearance c of the perceived corridor between two detected objects is calculated as the sum of the distances $dist_l$ and $dist_r$ perpendicular to S_{front} (cf. Fig. 2(a)). c is then reduced by a gap g to account for a pedestrian's tendency to exaggerate the body rotation while navigating through a narrow space

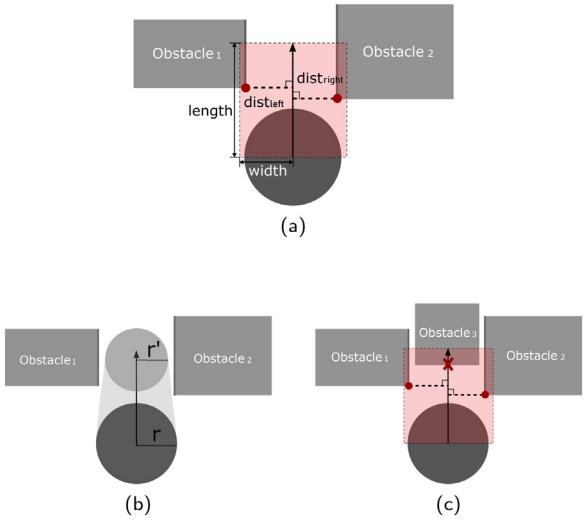

Fig. 2. Size adaptation when traversing a narrow corridor. (a) shows an agent detecting the clearance between two obstacles in front. (b) shows an agent adjusting its size to the perceived corridor. (c) shows an exceptional case where the detected corridor is obstructed.

Table 1
Sum of width and maintained gap in corridors computed based on the empirical data.

Corridor width (m)	0.6	0.7	0.8	0.9	1.0
Sum of width (m)	0.6	0.678	0.758	0.846	0.944
Gap (m)	0	0.022	0.042	0.054	0.056

in order to maintain a non-zero distance to the walls or neighbors. The preferred radius of the agent can then be calculated as $\frac{1}{2}(c-g)$.

The value of g is determined as a function of c, which is calibrated using the data from the mock up experiment of a similar corridor scenario carried out by Yamamoto et al. [30]. Pairs of participants asked to start from the opposite sides of the corridor. Each participant was equipped with a gyro sensor which was able to record the angular velocity of the participant's body rotation. The maximum rotation angle during the procedure could be acquired using integration. The length of the space occupied by each participant in the direction of the corridor width was computed using the maximum rotation angle during interaction, denoted by w_i and w_j (cf. Fig. 1(a)). Finally, the sum of widths $w_s = w_i + w_j$ was computed. We rely on w_s to determine the gap g for a given clearance c (cf. Fig. 1(b)).

As suggested in [4,30], the average shoulder width is around 0.5 m and the average chest width is around 0.3 m. We therefore use 0.25 m as the maximum radius (shoulder radius) and 0.15 m as the minimum radius (chest radius) of an agent. In this case, the narrowest corridor which two agents in our model can navigate through together laterally is therefore 0.6 m. As a result, we assume $g = 0$ in 0.6-m corridor scenarios. And on the other hand, the agents no longer need to adjust their size if the corridor is wider than 1 m. We are therefore only interested in the empirical data with $w = 0.6, 0.7, 0.8, 0.9$ and 1.0 m.

Yamamoto et al. also point out that, due to the insufficient wall height (62 cm), the participants were able to put their upper bodies over the corridor [30]. However, in our simulation tool, agents are not allowed for overlapping any obstacles. We therefore filtered out those data with w_s larger than the given corridor width.

As shown in Table 1, the resulting gap g is heavily dependent on the corridor width. In particular, even in a 1m wide corridor, where two participants could pass each other without any rotation, a gap of 0.056 m can still be observed. As shown in Fig. 3, we determine the relation between the preserved gap and the clearance under the

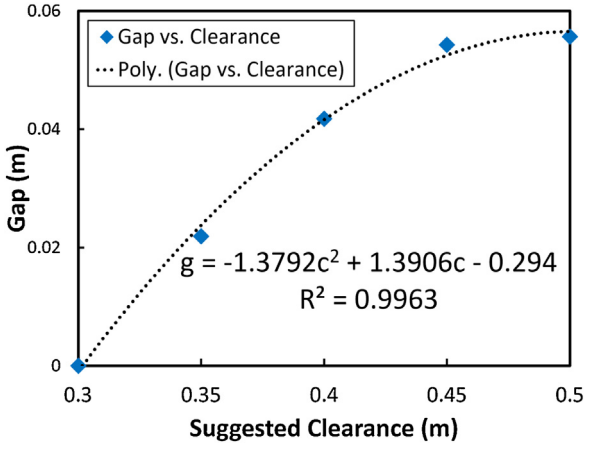

Fig. 3. Data fitting graph of gap and clearance.

Table 2
Average error of travel time (%) for each combination of α and β. The minimum value and the corresponding parameter pair are highlighted.

α	β					
	0.5	0.6	**0.7**	0.8	0.9	1.0
0	1.63	1.29	0.97	0.60	0.26	0.11
0.025	1.31	0.94	0.49	0.26	0.13	0.15
0.050	0.52	0.57	0.24	0.21	0.16	0.32
0.075	0.49	0.27	**0.07**	0.12	0.18	0.47
0.100	0.30	0.23	0.11	0.09	0.30	0.79
0.125	0.26	0.20	0.10	0.19	0.35	0.99

assumption that each agent perceives half of the corridor width as clearance. We used quadratic regression to fit the data, acquiring a R-square value close to 1, indicating a good fit.

3.1.2. Speed adjustment

In addition to the dynamic change of body size, adjustment of preferred walking speed is also introduced for the first time in our model. Exiting works [3,30] highlight the deceleration of pedestrians while rotating or shrinking. Borrowing the idea from [3], the preferred speed of an agent s^0 can be represented as follows:

$$s^0 = s^0_{\max}\left[\frac{(r^0-\alpha)}{(r_{\max}-\alpha)}\right]^{\beta}$$

where α and β are two constant values to be calibrated.

Using the gap maintenance model, we calibrated the α and β using the data from [30] by replicating the mock-up experiment with corridor width from 0.7 to 1.0 m (4 scenarios in total). We varied α from 0 to 0.125 with interval 0.025 and β from 0.5 to 1 with interval 0.1, and for each combination 20 iterations were performed. The travel time within the 2-m region in the corridor center were measured. The average travel time of a scenario among 20 iterations is denoted by T_n, where n is the scenario index.

To select the best combination of the parameters, for each pair of α and β, the error E was computed by:

$$E = \frac{1}{N}\sum_{n=1}^{N}\left|\frac{T_n-\overline{T}}{\overline{T}}\right|$$

where N is the number of scenarios and $\overline{T}$ is the average travel time of the scenario from empirical data. The results were shown in Table 2, suggesting that the best combination is α = 0.075 and β = 0.7.

3.2. Collision prediction

The size adaptation behavior provides a possibility for the agents to pass. However, without changing the desired walking direction, the current model still fails to eliminate head-on collisions. The right-of-way behavior [12] is not functional here because both pedestrians share an equal priority level. In fact, even in more general cases, SFM does not guarantee the collision-free movement unless the repulsive force from the opponent is large enough. However, simply increasing the force will lead to an excessive personal space preservation, making it difficult to navigate in a confined environment.

To address this issue, we propose a simple collision prediction (CP) method to adjust the desired walking direction of agents when given a potential collision within a certain number of time steps. From the perspective of agent i, his desired velocity V_i^0 is known and the instantaneous velocity V_j of the neighboring agent j is perceivable (the desired velocity of j is inaccessible to i). The distance between agent i and agent j predicted by i at a future time $t + \Delta t$ can therefore be represented as:

$$D(t + \Delta t) = ||(P_i(t) + V_i^0 \Delta t) - (P_j(t) + V_j \Delta t)||$$

We use t_m to denote the time when $D(t)$ reaches the minimum value.

Given the radius of two agents r_i and r_j, a potential collision is detected if $0 \leq D(t_m) < r_i + r_j$. In a general cases where $D(t_m)$ is less than $r_i + r_j$, agent i appends an escape velocity v_e to the initial desired velocity v_i^0. v_e consists of $v_{e,n}$ in normal direction lying on the common chord l of the agents, and $v_{e,t}$ in tangential direction lying on the distance vector between the agents (cf. Fig. 4(a) and (b)). The common chord l can be computed as followed:

$$l = \begin{cases} \sqrt{r_i^2 - \left(\dfrac{D(t_m)^2 - (r_i^2 - r_j^2)}{2D(t_m)}\right)^2} & 0 < D(t_m) < r_i + r_j \\ 0 & D(t_m) >= r_i + r_j \\ 2r_i & D(t_m) = 0 \end{cases}$$

We assume that both agents would share the responsibility of avoiding collision equally as [29] suggested. The magnitude of $v_{e,n}$ is equal to $l/2$ and the that of $v_{e,t}$ is equal to $(r_i + r_j - D(t_m))/2$.

In particular, when $D(t_m) = 0$, indicating an exact head-on collision, the escape velocity v_e cannot be computed following the definition above (cf. Fig. 4(c)). In this case, $v_{e,n}$ is set as a vector perpendicular to v_i^0 with the magnitude equal to $l/2$, while $v_{e,t}$ is set to be 0.

In order to maintain the magnitude of the desired velocity, the new desired velocity $v_i^{0'}$ is normalized against the initial desired velocity v_i^0, i.e., $v_i^{0'} = (v_i^0 + v_e)/||v_i^0||$.

Although we present the collision prediction method with a head-on collision situation, the method is not limited to this kind of scenarios. It can also be used in more general cases, e.g., an agent adjusting his velocity to overtake someone in front walking in lower speed (cf. Fig. 4(d)). Note that here we only focus on the interaction between agents. As collisions with obstacles are not predicted, their avoidance relies purely on the SFM.

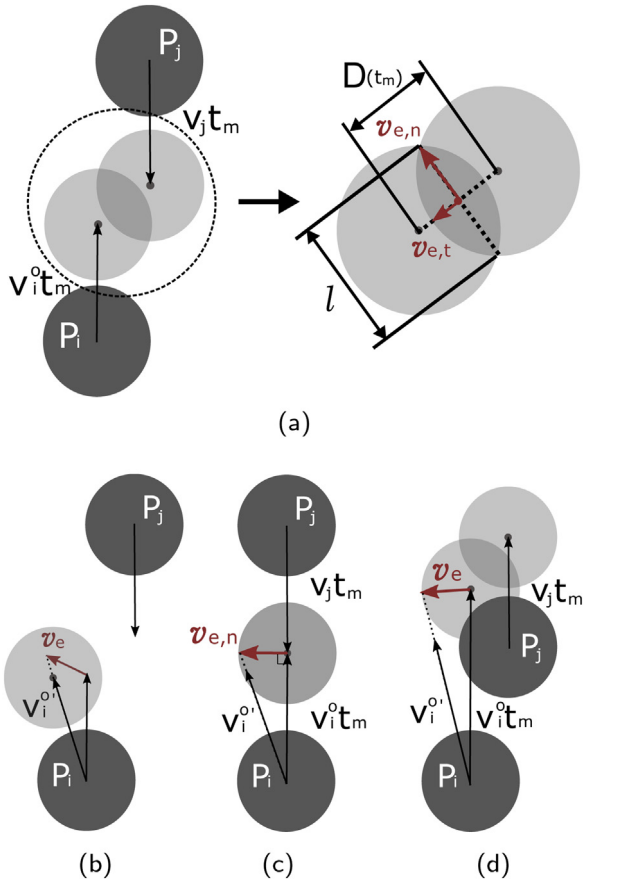

Fig. 4. Collision prediction behavior of agents. The left figure in (a) shows a collision predicted by agent i. The right side demonstrates the escape velocity $v_{e,n}$ and $v_{e,t}$. (b) shows the adjusted velocity of agent i. Agent j will also have the opposite adjustment. (c) shows the v_e computed for an exact head-on collision. (d) shows the overtaking behavior of agent i.

4. Scenario

In the following, we describe the scenario considered in our simulations. The AV layout is provided as a color-coded 2D floor plan. As shown in Fig. 5, each layout represents a 6 m × 6 m station comprised of the vehicle of size 6 m × 2.7 m, and the platform (6 m × 3.3 m). The interior region includes regular seats and leaning seats (where passengers can lean on the wall), seat areas, standing

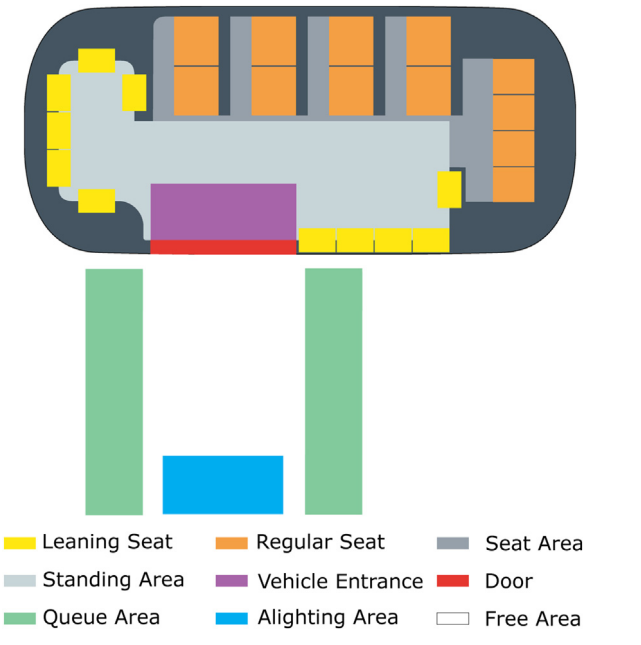

Fig. 5. Color-coded autonomous vehicle layout used as input to the simulation.

Table 3
The experience set of a boarding passenger.

Experience	Stage	Action
QueueExp	Queue	WaitAtPoint
GetOnVehicleExp	GoToDoor	Navigate
	GoToVehicleCenter	StraightWalk
GoToSeatExp	GoToSeatCenter	Navigate
	ArrivedSeat	Still
GoToStandingAreaExp	GoToStandingPoint	Navigate
	IdleInStandingPoint	WaitAtPoint

areas, and a door. Outside the vehicle, queue areas and an alighting area are specified. Alighting passengers are assumed to exit the scenario through the alighting area. To simplify the boarding process, a vehicle entrance is defined as the position at which boarding agents choose their preferred destination.

We assume that when the simulation starts, the AV has stopped at the station and passengers are queuing at the platform. A configurable number of passengers then exits the vehicle, while some are assumed to stay inside to continue their trip. Once all alighting passengers have exited, the queuing passengers board the vehicle and move to their preferred seats or a location in the standing area. We are interested in the times taken for all alighting passengers to exit the vehicle and for the boarding passengers to enter the vehicle and to reach their desired locations.

5. Passenger model

In this section, we describe the high-level decision-making and low-level distance-keeping behavior of our agent-based passenger model. Due to the highly confined environment within the vehicle, our model must address two main challenges: firstly, passengers must be able to pass through corridors narrower than their shoulder width. Secondly, the model must be able to cope with passenger passing each other in confined areas. We developed the model in the CrowdTools [8] simulation framework, which is an implementation of the RPD paradigm (cf. Section 2).

5.1. High-level decision making

The high-level decision making process determines a target destination and a desired status of an agent, including preferred speed, preferred walking direction and preferred radius. These targets and preferences are achieved through the selection of suitable behaviors via the RPD framework and supported by dynamic size adaptations and collision prediction.

5.1.1. Behavior selection

There are three types of agents in our model:

- **Alighting passengers (AP):** APs are created in a seat or in the standing area and cross the vehicle center to reach the door. After exiting the vehicle, APs enter the alighting area to disappear from the scene.
- **Boarding passengers (BP):** BPs are generated within the queue areas and start to board. After subsequently entering the vehicle, each BP chooses a standing point or a seat. Once the desired location has been reached, the BPs become passive.
- **Passive passengers (PP):** PPs are generated uniformly at random inside the vehicle, occupying a seat or space for standing. Larger numbers of PPs increase the interior density and prolong the boarding and alighting process.

Since the behavior of APs and PPs is relatively simple, our description focuses on the BP behavior. Table 3 lists the action to be executed in each stage in the experience set of BPs: *Navigate* represents long-distance navigation based on the approximated best-first search A^* algorithm [8]; *StraightWalk* represents direct translation only used on unobstructed paths; *WaitAtPoint* represents idling at the waiting point and returning to the position when being pushed away by neighbors; *Still* represents standing at the current position.

Fig. 6 shows an excerpt of the decision-making when a BP arrives at the vehicle center, restricted to one stage for each experience. The BP first determines the experience that best matches the cue "Priority to Seats", which is "Go to seat". While the agent carries out the associated action of navigating to the seat, its perception system continuously evaluates the remaining distance and the occupation to the target seat. A violation of the agent's expectations is detected if the target is no longer available. The agent's current goal is considered to be achieved once the agent enters the seat. When an agent exits the current stage after having achieved the associated goal, it enters the subsequent stage of the current experience. In contrast, when the agent exits the stage through a violation of its expectations, a new round of experience matching is triggered.

5.2. Low-level collision avoidance

We rely on the social force model (SFM) with right-of-way extensions (cf. Section 2) for the fundamental collision-avoidance behavior among agents. To achieve plausible agent behavior in the confined environment of our boarding and alighting scenario, we propose three modifications to the model.

5.2.1. Force reduction

The magnitudes of the forces generated by the original SFM are excessive when considering confined scenarios, where passengers may stand nearby each other or pass other passengers at close distances, while still aiming to avoid potential collision. This is contrary to the common use cases of SFM in large-scale scenarios with open spaces, where pedestrians tend to maintain relatively large distances from each other. Further, in our scenario, strong repulsive forces from stationary obstacles make it impossible for agents to traverse the seat edge areas and to enter seats.

We assume that passengers tend to maintain smaller distances to objects nearby within the vehicle than in an open space, and that they keep larger distance from neighboring passengers than from stationary obstacles. Although reducing the agent size makes it possible for agents to traverse paths that are narrower than their shoulder width, they may still fail to enter a corridor because of the strong repulsive force from the corridor walls. We address this issue by reducing the forces using two new scaling factors λ_{agent} and λ_{obs}:

$$m_i \frac{\mathrm{d}v_i}{\mathrm{d}t} = m_i \frac{v_i^0(t) - v_i(t)}{\tau_i} + \lambda_{agent} F_{nb} + \lambda_{obs} F_{obs}$$

We assign λ_{agent} and λ_{obs} values between 0 and 1. Reducing these forces also enables agents to stand both closer to each other and closer to walls, which is necessary to achieve high passenger densities commonly observed in public transport situations. In our simulation experiments, the specific values for the scaling factors were hand-tuned based on visual inspection of trial simulations, with values adapted according to the area in which each agent currently resides. The specific values are given in Section 6.

5.2.2. Modification of right-of-way behavior

We employ an existing extension to the SFM that relies on agent priorities to model right-of-way behavior [12]. Three levels of the agent priority p are defined in our model. All types of agents start with an initial p value of 0. During the simulation, APs and BPs increase their priority to 1 when they are navigating inside the vehicle, and reset the value when they exit the vehicle or reach

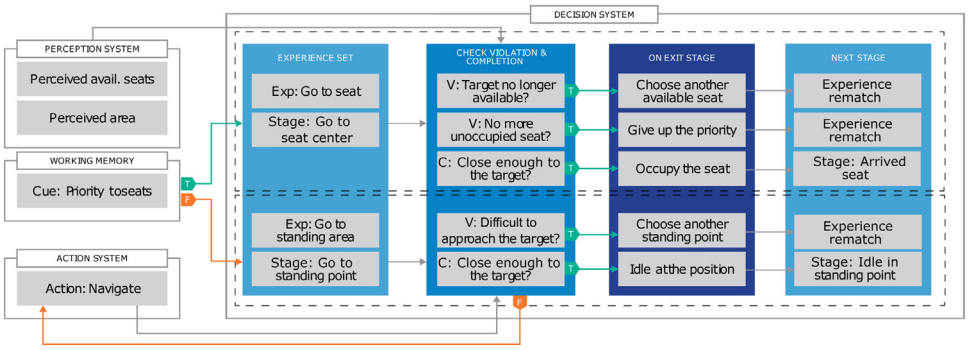

Fig. 6. An excerpt of the decision making of a boarding passenger when determining the next action after entering the vehicle.

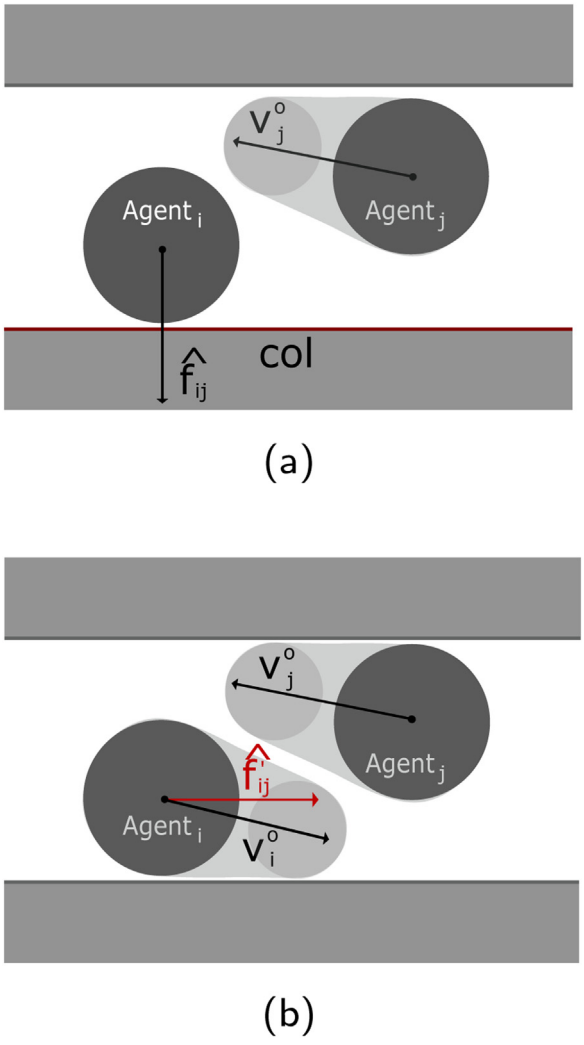

Fig. 7. (a) is the illustration of a situation that cannot be resolved by the original right-of-way SFM. (b) shows a solution by adjusting the repulsive force.

their destination inside the vehicle. An agent i with priority equal to 0 yields to another agent j with higher priority by moving in the direction perpendicular to the walking direction of j. For all agent types, p is set to -1 when the agent is seated. An agent with negative priority does not receive any social force, ensuring that the agent retains its position.

In certain situations, the above behavior fails to allow agents to pass each other successfully. For example, as shown in Fig. 7a, the agent j is moving ahead in a narrow corridor, while the standing neighbor agent i of lower priority is blocking the way. When the repulsive force $\hat{f}_{ij}$ is pointing to an obstacle, agent i has no space to step backward. The shrinking behavior of agent i will not be triggered since his velocity is also pointing to the obstacle due to the force. Although in the meantime agent j is able to adjust his desired velocity v_j^0 by collision prediction and execute size adaptation as usual, he will fail to go through the gap that is smaller than his minimum body size.

We have presented a quick solution on this special case in our previous work [27] by reorienting $\hat{f}_{ij}$. To detect the situation, an extra step is added during the agent force computation: The agent first perceives the distance to the closest obstacle line *col*. If the distance only exceeds the agent's radius by a small positive ϵ, we assume that the agent cannot give way to its neighbor. In this case, the repulsive force is reoriented to $\hat{f}'_{ij}$, parallel to *col*, which makes executing the collision prediction and size adaptation become possible to agent j. Both agents will eventually solve the collision by adjusting their walking direction and body size (cf. Fig. 7(b)).

6. Evaluation

In this section, we present the validation of our model against results from real-world experiments from the literature. Further, we demonstrate the practical use of the model by comparing the boarding and alighting times required by different layouts of an autonomous vehicle created by industrial designers.

6.1. Parameter setup

In Section 5, we described our adaptations of the social force model to allow passengers to navigate the confined space inside the vehicle. To reduce the intensity of the forces from other agents and obstacles inside the vehicle, the scaling parameters are configured as follows for agents outside the vehicle, inside the vehicle, and on the seat edge: $\lambda_{agent} = 0.8, 0.6, 0.2$; $\lambda_{obs} = 0.2, 0.1, 0.01$. To retain the distance kept by passengers even in confined spaces, the force generated by obstacles is reduced more sharply than that of agents. While our model allows modelers to specify passenger personas defined by preferred walking speeds and seat selection preferences, here we assume all passengers to be working adults, with a preferred speed of 1.4 m/s outside the vehicle, which is reduced to 0.56 m/s inside the vehicle, and to 0.28 m/s in the seat edge area. Seat selection is assumed to be uniformly at random. We are investigating approaches for data collection from virtual reality experiments [2] and real-world experiments to support the representation of different passenger types.

6.2. Validation experiment

In 2010, Fernández et al. carried out experiments on the influence of the platform and vehicle design on boarding and alighting times as well as passenger saturation flows of a public trans-

Table 4
Validation results.

Scenario and metric	Empirical	Without CP	With CP	Restricted CP ($n = 5$)	Previous model
Wide door, average alighting time	0.73 s/pass	0.97 s/pass	0.53 s/pass	0.75 s/pass	0.81 s/pass
Narrow door, average alighting time	1.22 s/pass	1.41 s/pass	0.91 s/pass	1.19 s/pass	1.23 s/pass
Narrow door, alighting saturation flow	0.85 pass/s	0.97 pass/s	1.36 pass/s	0.87 pass/s	0.83 pass/s
Narrow door, average boarding time	1.54 s/pass	1.59 s/pass	1.16 s/pass	1.58 s/pass	1.56 s/pass
Wide door, average boarding time	1.18 s/pass	1.28 s/pass	0.58 s/pass	1.22 s/pass	1.22 s/pass

port vehicle [18,15]. The participants of the experiment repeatedly boarded or alighted a full-scale mock-up. In our original conference paper, we recreated the vehicle layouts used in the real-world experiments in our simulation and validated our model by comparing the results from these experiments to ours. Here, we repeat the same validation process with our new model.

We first performed experiments with and without the collision prediction component. Due to the reduced shrinking extent and the deceleration behavior in the size adaptation, the boarding and alighting times were longer than with our previous model. On the other hand, enabling the collision prediction behavior led to a substantially faster boarding and alighting process, in which all agents were seeking opportunities to overtake their neighbors in front (Table 4).

We notice that the effect of collision prediction (CP) can be controlled by restricting the triggering condition, that is, to perform CP only when the number of neighbors perceived by an agent is less than a certain value n. The value was configured using the wide door alighting scenario. For an agent with a perception range of one meter, choosing $n = 5$ achieved results closest to the empirical data. The validation was carried out in other scenarios using the restricted collision prediction behavior. As shown in Table 4, the observed deviations lie between 2% and 6%, representing a slight average improvement over our results in the previous paper. As a consequence, we consider the new model accurate enough to provide estimates of real-world boarding and alighting times.

6.3. Case study

We demonstrate the practical use of our model by evaluating the times taken for the boarding and alighting process when considering three different autonomous vehicle layouts. The following metrics are considered:

- **Alighting time:** The time until alighting passengers have exited the vehicle.
- **Boarding time:** The time until all alighting passengers have exited and all boarding passengers have entered the vehicle.
- **Settling time:** The time at until all boarding passengers have settled on a seat or in the standing area.

The effect of the settling time on the required dwell time depends on the point in time when the vehicle starts its trip. Although the vehicle could start its trip as soon as all passengers have entered the vehicle, considerations of passenger comfort may suggest a delay to allow passengers to take their seats.

Fig. 8 shows the interior layouts to be evaluated. Two of the layouts represent extreme cases with respect to the seat numbers and thus passenger comfort: “standing only” does not provide any regular seats, leaving a large amount of space for navigation inside the vehicle, whereas “maximum seating” provides 16 seats in total. The layout “balanced” aims to provide a sufficient number of seats, while still allowing passengers to navigate comfortably. Further, the layout leaves space near the door to place a wheelchair.

We separated the case study into low-density cases and high-density cases. For low-density cases, we populated each layout with 6 alighting passengers (3 sitting and 3 standing), 6 passive passengers (3 sitting and 3 standing), and 6 boarding passengers. 100 iterations were executed for each layout.

Table 5
Average times in low density cases.

Layout	(a)		(b)		(c)	
Impatient BPs	N	Y	N	Y	N	Y
Alighting time (s)	6.0	9.7	6.8	9.1	6.2	9.6
Boarding time (s)	11.2	17.3	12.3	16.0	11.7	16.3
Settling time (s)	16.3	21.7	20.0	22.8	18.3	21.8

It is worth pointing out that, in our previous study, we assumed that BPs would wait outside the AV until all the APs have alighted, while here we assume that BPs are all impatient and will start boarding at the beginning of simulation.

For the high-density cases, we populated each layout with a sufficient amount of PPs to fill the standing space (i.e., the standing area and vehicle entrance), leaving one seat for a sitting passenger about to alight.

6.3.1. Low-density scenarios

The frequency and average values of three metrics are presented in Figs. 9 and 10 and Table 5. The results without impatient boarding passengers indicate that the layout “standing only” allowed for the shortest alighting, boarding, and settling times. The layout “maximum seating” yielded the largest values for all three metrics, while times taken with the “balanced” layout are in between of those taken with the other two layouts, due to its medium-sized navigation space.

Compared to the results of our previous study [27], we observe that the values of most metrics slightly reduced. This can be attributed to the collision prediction behavior, which allows the passengers to navigate through the crowd more easily.

On the other hand, the results with impatient boarding passengers show much less difference between the three layouts on all of the metrics. The layout “standing only” suffers a great increase on all three processing times: alighting time increasing by 61.2%, boarding time increases by 54.2%, and settling time increases by 33.1%. The layout “balance” is slightly better than that the “standing only”, with alighting time increasing by 54.8%, boarding time increases by 39.3%, and settling time increases by 19.1%.

The layout “maximum seating” is the least influenced, with alighting time only increasing by 33.8%, boarding time increases by 30.1%, and settling time increase by 14.0%. One possible reason for the differences in the increase is that the aisles at seat areas can somewhat reduce the alighting flow, and therefore minimize the conflicts between APs and BPs at the vehicle entrance area.

6.3.2. High-density scenarios

To achieve a highly dense environment, passive passengers were inserted to fully occupy the seats and standing areas, leaving only one empty seat for an alighting passenger. The layout “standing only” contains 29 standing PPs, the layout “maximum seating” contains 10 standing PPs, and the layout “balanced” contains 16 PPs, resulting in crowd densities of 63.1%, 61.7%, and 61.7% (the density is measured using the ratio of standing space occupied by the

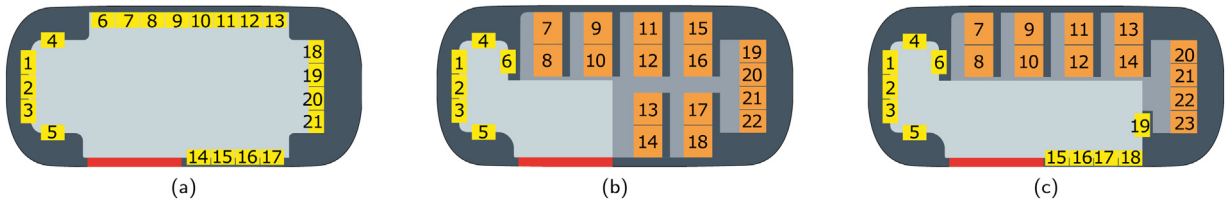

Fig. 8. Autonomous vehicle interior layouts evaluated in the case study. (a) Standing only: no regular seats, maximizing space for movement; (b) maximum seating: maximizing the number of regular seats; (c) balanced: regular seats while preserving space for movement.

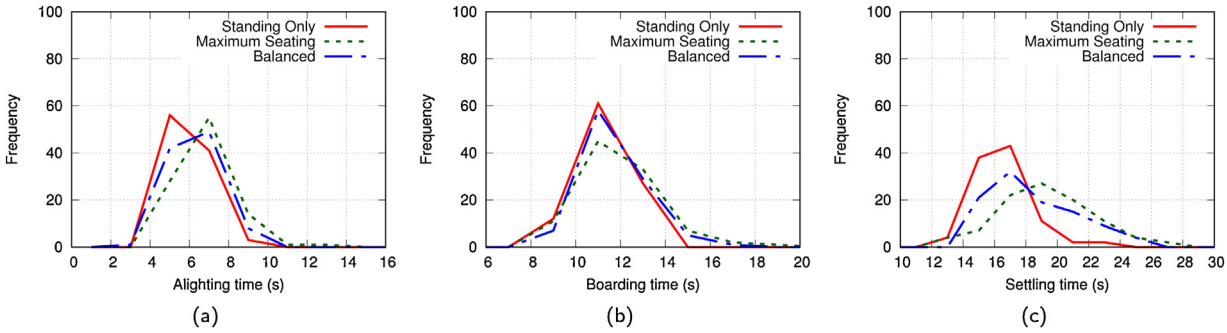

Fig. 9. Simulation results for the three layouts in the low density cases with no impatient boarding passengers.

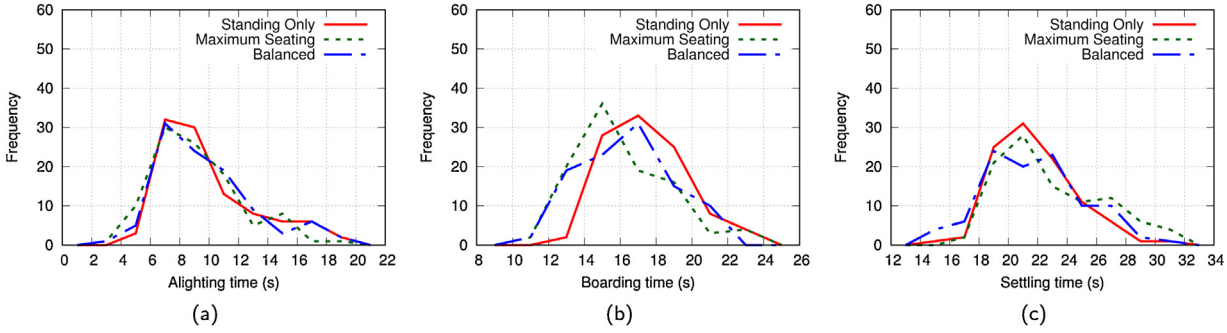

Fig. 10. Simulation results for the three layouts in the low density cases with all impatient boarding passengers ($n = 6$).

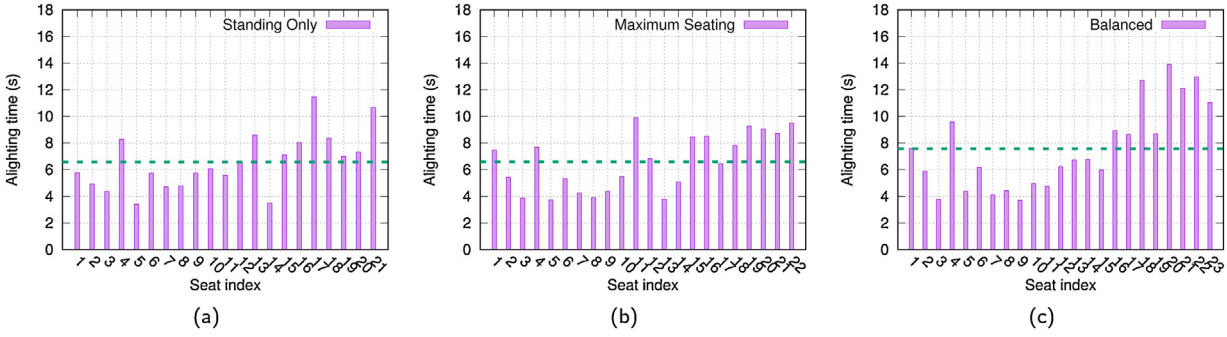

Fig. 11. Simulation results for the three layouts in the high density cases. The green dash lines show the average alighting times of all the seats. (For interpretation of the references to color in this figure legend, the reader is referred to the web version of this article.)

circles). 20 iterations were performed for each seat and the average alighting times of the only alighting passenger are measured to determine the quality of seat placement. Here we only interested in the alighting process since simulating the inverse process will probably produce similar results.

The results shown in Fig. 11 indicates that, in general, the required alighting time from a seat has a strong relationship with the distance to the door (compare, for instance, seats 14 and 18 in the layout "standing only"). Alighting from the seats next to corners is more time consuming than from the ones in the middle (e.g., seats 13 and 17 in the layout "standing only").

The alighting process from a random seat in the layout "standing only" required the shortest time among the three layouts, with average of 6.57 s. The average alighting time for the layout "maximum seating" was 6.77 s, slightly longer than for the layout "standing only". The layout "balanced" generated the largest alight

times among all, 7.57 s on average. Particularly large values can be observed at the seats 20, 21, 22 and 23. By reviewing the simulation traces, we noticed that the alighting passengers from those seats had a high probability to be blocked by standing passengers at the aisle between seats 14 and 19, which forms a bottleneck. Another particularly large value can be observed for seat 18, which is located at the corner. These observations suggest that the layout "balanced" could possibly be improved by removing seat 19 to maintain a wider aisle for the rear seats and more space for seat 18.

According to our simulation-based evaluation, the lowest boarding, alighting, and settling times are achieved with the layout "standing only". Of course, while the purely quantitative evaluation permits comparisons in terms of efficiency, it must also be ensured that the selected layouts satisfy other requirements such as those given by Universal Design principles [10], as well as service quality indicators for public transportation as defined by standards such as EN 13186 [14].

7. Conclusion and future work

We presented a novel passenger model for evaluating public transport vehicle layouts in terms of the required dwell time. The low-level model is based on the traditional SFM with additional right-of-way features. The high-level model is based on the RPD framework used to define the passenger behavior, allowing for an adaptive decision-making based on the current situation faced by agents.

In this extended version of the paper, we proposed a size adaptation model for circular agents to achieve collision avoidance in narrow corridor scenarios with multiple agents. Gap maintenance behavior and walking speed adjustments were introduced and calibrated using empirical data in order to fully emulate the rotation behavior of human passengers. Adjustments to the desired walking direction via a collision prediction mechanism was introduced to allow passengers to passing each other successfully. The size adaptation model was integrated as part of the high-level behavior of our passenger model.

We validated the new model by replicating a mock-up experiment from the literature in our simulation. The observed deviations in boarding and alighting times were below 6%. Further, we applied our simulation to autonomous vehicle layouts created by industrial designers, demonstrating substantial differences in the dwell times depending on the number of seats and their positioning. By relying on color-coded floor plans as the input to the simulation, different vehicle layouts can be evaluated easily. Of course, apart from efficiency metrics such as the dwell time, viable vehicle designs must also be evaluated in terms of the provided service quality through features such as step-free access, space for wheelchair users, and the presence of handrails.

In future work, we aim to extend our experiments to passengers with different characteristics. To this end, we are exploring data collection from virtual reality experiments [2] and real world observations. The empirical data will reveal the seat selection of different personas and also more realistic passenger placement in the module (e.g., alighting passengers standing up and queuing in front of the exit) when the vehicle stops.

Potential future refinements include more complex passenger interactions in confined environments (e.g., exiting the vehicle to allow passengers to alight), joint decision-making (e.g., assisting elderly people), and crowd mixes at specific times of day (e.g., during peak hours). More dynamic agent perception will be introduced such as inattentive agents (alighting passengers that realize their arrival later than others) and less collision-sensitive agents (e.g., passengers distracted by their phones).

Authors' contribution

Boyi Su: methodology, conceptualization, software, validation, writing – original draft, writing – review & editing. Philipp Andelfinger and Jaeyoung Kwak: methodology, conceptualization, writing – review & editing. David Eckhoff: project administration, supervision, methodology, writing – review & editing, conceptualization. Henriette Cornet: project administration, resources. Goran Marinkovic: resources, visualization. Wentong Cai: supervision, project administration, writing – review & editing. Alois Knoll: project administration.

Conflict of interest

None declared.

Acknowledgment

This work was financially supported by the Singapore National Research Foundation under its Campus for Research Excellence And Technological Enterprise (CREATE) program.

References

[1] F. Alonso-Marroquin, J. Busch, C. Chiew, C. Lozano, A. Ramírez-Gómez, Simulation of counterflow pedestrian dynamics using spheropolygons, Phys. Rev. E 90 (2014) 063305.
[2] P. Andelfinger, D. Zehe, Y. Chen, B. Su, D. Eckhoff, W. Cai, A. Knoll, Incremental calibration of seat selection preferences in agent-based simulations of public transport scenarios, in: Proceedings of the Winter Simulation Conference (WSC), Gothenburg, Sweden, 2018, pp. 833–844.
[3] G. Baglietto, D.R. Parisi, Continuous-space automaton model for pedestrian dynamics, Phys. E 83 (2011) 056117.
[4] A. Best, S. Narang, D. Manocha, Real-time reciprocal collision avoidance with elliptical agents, 2016 IEEE International Conference on Robotics and Automation (ICRA) (2016) 298–305.
[5] B. Bian, N. Zhu, S. Ling, S. Ma, Bus service time estimation model for a curbside bus stop, Transp. Res. Part C: Emerg. Technol. 57 (2015) 103–121.
[6] N.W.F. Bode, A.U.K. Wagoum, E.A. Codling, Human responses to multiple sources of directional information in virtual crowd evacuations, J. R. Soc. Interface 11 (2014) 20130904.
[7] D.A. Bowman, R.P. McMahan, Virtual reality: how much immersion is enough? Computer 40 (2007) 36–43.
[8] W. Cai, S. Zhou, M. Low, F. Tian, H. Seah, D. Ong, V. Tay, B. Hamilton, L. Luo, D. Wang, K. Sornum, M. Lees, Z. Shen, D. Chen, X. Xiao, A. Liang, M. Xiong, COSMOS: CrOwd Simulation for Military Operations. Technical Report, School of Computer Eng., Nanyang Technological University, Singapore, 2010.
[9] M. Chraibi, A. Seyfried, A. Schadschneider, Generalized centrifugal-force model for pedestrian dynamics, Phys. Rev. E 82 (2010) 046111.
[10] B.R. Connell, M. Jones, R. Mace, J. Mueller, A. Mullick, E. Ostroff, J. Sanford, E. Steinfeld, M. Story, G. Vanderheiden, The Principles of Universal Design, 1997 https://projects.ncsu.edu/www/ncsu/design/sod5/cud/about_ud/udprinciplestext.htm.
[11] S. Curtis, S.J. Guy, B. Zafar, D. Manocha, Virtual Tawaf: a case study in simulating the behavior of dense, heterogeneous crowds, in: International Conference on Computer Vision Workshops, Barcelona, Spain, 2011, pp. 128–135.
[12] S. Curtis, B. Zafar, A. Gutub, D. Manocha, Right of way: asymmetric agent interactions in crowds, Visual Comput. 29 (2013) 1277–1292.
[13] T. Elliott, Expert Decision-Making in Naturalistic Environments: A Summary of Research, 2005, pp. 70.
[14] European Committee for Standardization, Transportation – Logistics and Services – Public Passenger Transport – Service Quality Definition, Targeting and Measurement. Standard EN, 2002, pp. 13816.
[15] R. Fernández, P. Zegers, G. Weber, N. Tyler, Influence of platform height, door width, and fare collection on bus dwell time: laboratory evidence for Santiago de Chile, Transp. Res. Rec.: J. Transp. Res. Board (2010) 59–66.
[16] D. Fletcher, R. Harrison, T. Karmakharm, S. Nallaperuma, P. Richmond, RateSetter: roadmap for faster, safer, and better platform train interface design and operation using evolutionary optimisation, in: Proc. of the Genetic and Evolutionary Computation Conference, ACM, Kyoto, Japan, 2018, pp. 1230–1237.
[17] Y. Gao, P.B. Luh, H. Zhang, T. Chen, A modified social force model considering relative velocity of pedestrians, in: International Conference on Automation Science and Engineering (CASE), Wisconsin, USA, 2013, pp. 747–751.
[18] D. Helbing, P. Molnar, Social force model for pedestrian dynamics, Phys. Rev. E 51 (1995) 4282.

[19] G. Klein, The recognition-primed decision (RPD) model: looking back, looking forward, Nat. Decis. Making (1997) 285–292.
[20] P.A. Langston, R. Masling, B.N. Asmar, Crowd dynamics discrete element multi-circle model, Saf. Sci. 44 (2006) 395–417.
[21] N. Li, J. Huang, Y. Feng, K. Huang, G. Cheng, A review of naturalistic decision-making and its applications to the future military, IEEE Access 8 (2020) 38276–38284, http://dx.doi.org/10.1109/ACCESS.2020.2974317.
[22] L. Luo, S. Zhou, W. Cai, M. Lees, M.Y.H. Low, K. Sornum, HumDPM: a decision process model for modeling human-like behaviors in time-critical and uncertain situations, Transactions on Computational Science XII: Special Issue on Cyberworlds (2011) 206–230.
[23] S. Narang, A. Best, D. Manocha, Interactive simulation of local interactions in dense crowds using elliptical agents, J. Stat. Mech. Theory Exp. (2017).
[24] A. Perkins, B. Ryan, P.O. Siebers, Modelling and simulation of rail passengers to evaluate methods to reduce dwell times, in: 14th International Conference on Modeling and Applied Simulation, MAS 2015, Rende, Italy, 2015, pp. 132–141.
[25] M. Prédhumeau, J. Dugdale, A. Spalanzani, Adapting the Social Force Model for Low Density Crowds in Open Environments, 2019.
[26] S. Seriani, R. Fernandez, Pedestrian traffic management of boarding and alighting in metro stations, Transp. Res. Part C: Emerg. Technol. 53 (2015) 76–92.
[27] B. Su, P. Andelfinger, D. Eckhoff, H. Cornet, G. Marinkovic, W. Cai, A. Knoll, An Agent-Based Model for Evaluating the Boarding and Alighting Efficiency of Autonomous Public Transport Vehicles, Springer International Publishing, 2019, pp. 534–547.
[28] L. Sun, A. Tirachini, K.W. Axhausen, A. Erath, D.H. Lee, Models of bus boarding and alighting dynamics, Transp. Res. Part A: Policy Pract. 69 (2014) 447–460.
[29] J. Van Den Berg, S.J. Guy, M. Lin, D. Manocha, Optimal reciprocal collision avoidance for multi-agent navigation, in: Proc. of the IEEE International Conference on Robotics and Automation, Anchorage (AK), USA, 2010.
[30] H. Yamamoto, D. Yanagisawa, C. Feliciani, K. Nishinari, Body-rotation behavior of pedestrians for collision avoidance in passing and cross flow, Transp. Res. Part B: Methodol. 122 (2019) 486–510.
[31] Q. Zhang, B. Han, D. Li, Modeling and simulation of passenger alighting and boarding movement in beijing metro stations, Transp. Res. Part C: Emerg. Technol. 16 (2008) 635–649.

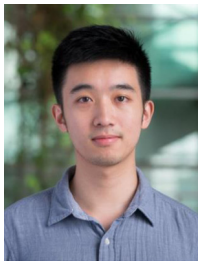

Boyi Su is a Research Associate in Complexity Institute at Nanyang Technological University (NTU). He received his master degree in school of Computer Science and Engineering in NTU, Singapore. His research interests are human behavior modelling and agent-based simulation.

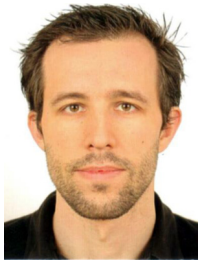

Philipp Andelfinger was a postdoctoral research fellow at TUMCREATE and Nanyang Technological University (NTU), Singapore in the group of Prof. Wentong Cai. He received his diploma and Ph.D. in Computer Science in 2011 and 2016 from Karlsruhe Institute of Technology (KIT), Germany.

Jaeyoung Kwak is currently a Research Fellow in Complexity Institute at Nanyang Technological University. He received his doctoral degree in transportation engineering from Aalto University, Finland. His research interests are primarily in pedestrian flow dynamics including data analysis, modeling, and numerical simulations.

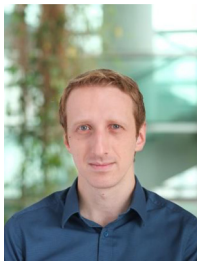

David Eckhoff is the principal investigator of the computer science group at TUMCREATE, Singapore, a joint research institute by TU Munich and Nanyang Technological University, Singapore. David received his Ph.D. degree in engineering and his M.Sc. degree in computer science from the University of Erlangen in 2016 and 2009, respectively. His research interests include privacy protection, smart cities, vehicular networks, and intelligent transportation systems with a focus on modelling and simulation.

Henriette Cornet graduated from the Technical University of Troyes, France, with a master's degree in Material Engineering in 2007. She received her doctoral degree from the Technical University of Munich in 2012. From 2011 to 2016, she worked as consultant for the automotive industry in Germany (BMW and Audi). Since 2017, she leads the team 'Design for Autonomous Mobility' at TUMCREATE, Singapore, a research institute that develops a new mobility system for public transport based on driverless vehicles. The research of her team covers the design of Autonomous Vehicles including Human–Machine Interfaces.

Goran Marinkovic graduated from the Faculty of Applied Arts and Design in Belgrade, Industrial Design department as top student of his generation. In 2008 he obtained a Master's degree from Domus Academy (Milan, Italy) and University of Wales (Cardiff, UK) and did his Master thesis on Car Design & Transportation. He graduated with distinction. His professional experience includes projects in fields of product and graphic design for various local and international companies and organizations. Goran holds 11 design awards and he participated in many international exhibitions. Interfaces.

Wentong Cai is a Professor in the School of Compute Science and Engineering (SCSE) at Nanyang Technological University (NTU), Singapore. He is a member of the IEEE and the ACM. He is an Associate Editor of the ACM Transactions on Modelling and Computer Simulation (TOMACS), an editor of the Future Generation Computer Systems (FGCS), and an editorial board member of the Journal of Simulation (JOS). His research interests are in the areas of Modelling and Simulation, and Parallel and Distributed Computing.

Alois Knoll is a professor of Computer Science at the Technical University of Munich (TUM) and a visiting Professor at NTU, Singapore. He received his diploma (M.Sc.) degree in Electrical/Communications Engineering from the University of Stuttgart and his Ph.D. degree in Computer Science from the Technical University of Berlin. He was a full professor at the University of Bielefeld until 2001. Since autumn 2001 he has been Between April 2004 and March 2006 he was Executive Director of the Institute of Computer Science at TUM.